

Cross-polarized wave generation in the UV region

Lorenzo Canova,¹ Stoyan Kourtev,² Nikolay Minkovski,² Rodrigo Lopez-Martens,¹
Olivier Albert,¹ and Solomon M. Saltiel^{2,*}

¹Laboratoire d'Optique Appliquée, ENSTA Paristech, Ecole Polytechnique, CNRS UMR-7639,
91761 Palaiseau Cedex, France

²Department of Quantum Electronics, Faculty of Physics, Sofia University, St. Kliment Ohridski,
5 J. Bourchier Boulevard, Sofia-1164, Bulgaria

*Corresponding author: saltiel@phys.uni-sofia.bg

Received July 1, 2008; revised August 25, 2008; accepted August 27, 2008;
posted September 5, 2008 (Doc. ID 98195); published October 7, 2008

We demonstrate experimentally the generation of cross-polarized femtosecond pulses in BaF₂ crystal in the UV region. We show that unsaturated cross-polarized wave generation in the UV is six times more efficient than in the visible region, and we deduce the corresponding wavelength dispersion of the third-order nonlinearity. © 2008 Optical Society of America

OCIS codes: 140.3610, 190.4720, 190.4380, 320.5540.

Cross-polarized wave (XPW) generation is now recognized as a reliable nonlinear optical tool for increasing the temporal contrast of near-IR femtosecond pulses up to 11 orders of magnitude [1,2]. A high temporal contrast is crucial for avoiding any preplasma formation during the interaction of ultra-intense femtosecond laser radiation with solid targets [3,4].

XPW generation is a four-wave mixing process governed by the anisotropy of the real part of the third-order susceptibility tensor of the nonlinear medium. This process is automatically phase matched and has proved to be efficient and robust in the IR [5] and visible [6] spectral ranges. Femtosecond excimer laser amplifiers are being developed as ultraintense femtosecond UV laser sources that could be advantageous in many applications (material processing, biomedicine, laser fusion, etc.). Contrast improvement of such sources is of importance, since amplified spontaneous emission in the UV is directly absorbed during laser-matter interaction. Avoiding preplasma formation in the UV region is therefore even more critical than in the IR. In this respect efficient XPW generation schemes in the UV are needed.

Another motivation for extending XPW generation to shorter wavelengths is for the purposes of measuring UV pulse durations. XPW complies with the requirements of an appropriate UV pulse diagnostic: it is efficient, achromatic, and intrinsically phase matched, and it generates a measurable signal wavelength (identical to the input one) easily discriminated from the input wavelength through its polarization. By this rationale, XPW should be compared with several other methods used to measure the temporal profile or contrast of UV pulses (two-photon excited fluorescence in alkali-earth fluoride crystals [7,8], self-diffraction, or cross-phase modulation). Successful demonstration of XPW frequency-resolved optical grating at 400 nm is reported in [9].

In this Letter, we present what we believe to be the first systematic experimental investigation of the XPW process in the near-UV region. From the measurements we can estimate the dispersion of the $\chi^{(3)}$ tensor in BaF₂.

The experimental setup is shown in Fig. 1. The driving source is a frequency-doubled colliding-pulse mode-locked dye laser in a 3 mm type I KDP crystal ($\lambda=310$ nm after the doubling, $\tau\approx 100$ fs, repetition rate 10 Hz). The pulses are focused ($f=300$ mm) into a 2 mm z -cut BaF₂ crystal (m3m point group) placed between crossed polarizers. BaF₂ has no linear optical activity nor birefringence. It is highly transparent in the UV, as it presents a cutoff at 135 nm, so even losses due to two-photon absorption are small. For comparison, measurements are also performed at the fundamental laser wavelength $\lambda=620$ nm by removing the KDP doubling crystal and UV filter and using a focal length of 450 mm.

To accurately quantify the increase in efficiency of XPW in the UV, we measured the XPW intensity as a function of input intensity and crystal orientation in both the UV and the visible regions. This approach yields two independent ways to measure the increase in efficiency, which can then be compared with a theoretical model.

XPW generation efficiency measurements as a function of input intensity and wavelength are presented in Fig. 2. To estimate the input intensity for each of the measurements, the spot sizes of the input beams [UV and VIS (visible)] were carefully measured. The ratio of the spot areas (VIS/UV) was found to be 2.17. Furthermore, pulse durations are identical for both wavelengths owing to second-harmonic generation (SHG) experimental conditions. The KDP crystal thickness is such that temporal walkoff causes narrowing of the spectrum that counteracts the $\sqrt{2}$ broadening owing to the SHG process.

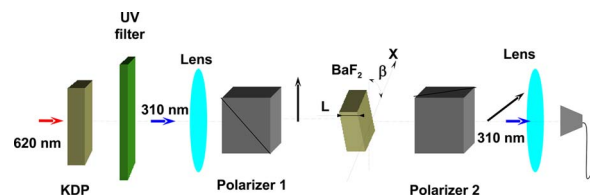


Fig. 1. (Color online) Schematic of the XPW experiment in UV region. BaF₂ is a z -cut sample. β is the angle between the x axis of the crystal and polarization plane of the input beam.

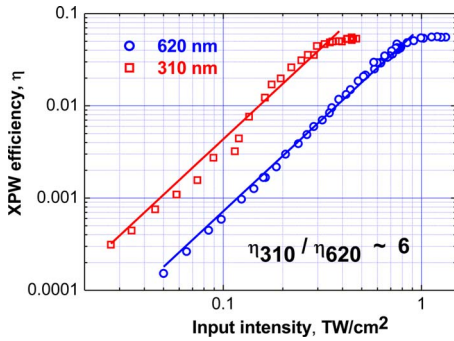


Fig. 2. (Color online) Comparison of cross-polarized wave efficiencies for the two input wavelengths indicated. The solid lines represent quadratic dependence.

The slope of XPW efficiency versus input pulse intensity follows a quadratic law, as expected from any cubic nonlinear process. For a given input intensity, XPW efficiency is six times higher in UV region when the nonlinear process is unsaturated. As seen from Fig. 2 the maximum achievable efficiency in UV is approximately the same as in the visible. Also, as the nonlinearity is higher in the UV, saturation, due to the dephasing between the fundamental and the XPW wave, occurs at lower input intensity compared to the saturation intensity for XPW generation in the visible region.

XPW efficiency being linked to the $\chi^{(3)}$ anisotropy, it is strongly dependent on the orientation of the crystal axes with respect to the input pulse polarization. Figure 3 shows the measured angular dependence of XPW efficiency at $\lambda=310$ nm $\lambda=620$ nm for input pulse energies $15.5\mu\text{J}$ and $56\mu\text{J}$, respectively. β is the angle between the input polarization plane and the crystal axis x . The latter energies correspond to intensities $465\text{GW}/\text{cm}^2 \pm 10\%$ at 310 nm and $780\text{GW}/\text{cm}^2 \pm 10\%$ at 620 nm, respectively.

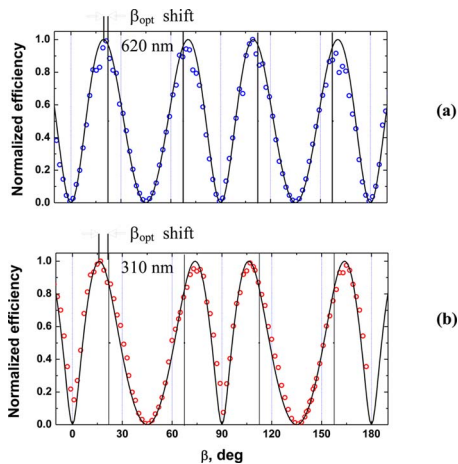


Fig. 3. (Color online) XPW generation efficiency as a function of the angle β for (a) 620 nm and (b) 310 nm fundamental wavelengths. Each of the experimental curves is normalized to the average value of the maxima. The lines are theoretical curves for Gauss/Gauss shapes for spatial/temporal modulation of the fundamental radiation for (a) $F=3.6$ and (b) $F=5.76$. The theoretical model used takes into account the processes of phase modulation of the interacting waves and depletion of the fundamental wave [6]. The vertical solid lines indicate optimal β position for low input intensities when $F \leq 1$.

Both dependencies shown on Figs. 2 and 3 enable us to estimate the increase in the third-order nonlinearity when changing the wavelength from 620 nm to 310 nm.

Let us first note that in the undepleted regime the XPW efficiency, η , is [6]

$$\eta = \frac{I_{\text{XPW}}}{I_0} = \frac{2}{\epsilon_0 c n} [(\sigma/4)\gamma_0 I_0 \sin(4\beta)L]^2, \quad (1)$$

where I_0 is input intensity, $\gamma_0 = 6\pi\chi_{xxxx}^{(3)}/8n\lambda$; L is the crystal length; and σ is the anisotropy of $\chi^{(3)}$ -tensor $\sigma = (\chi_{xxxx}^{(3)} - 3\chi_{xxyy}^{(3)})/\chi_{xxxx}^{(3)}$. Therefore, the origin of the dependence of η on wavelength is twofold. First, it presents a $1/\lambda^2$ dependence owing to the dispersion of γ_0 . Second, it is sensitive to the dispersion of product $\sigma\chi^{(3)}$.

We are able to measure the dispersion of $|\sigma(\chi_{xxxx}^{(3)})|$ and compare it with the existing data for the dispersion of $\chi_{xxxx}^{(3)}$. From this comparison, as will be seen below, we were able to draw conclusions about the dispersion of σ of BaF_2 .

From measurements presented in Fig. 2 and using Eq. (1), we obtain that $|\sigma(\chi_{xxxx}^{(3)})|$ is 1.22 times higher at 310 nm than at 620 nm. This is confirmed by the β scan analysis. XPW generation with high efficiency presents a β dependency that varies with the parameter $F = (2/\epsilon_0 c n)\sigma\gamma_0 I_0 L$, which can be understood as the B integral in the crystal [6]. When $F \ll 1$ the position of the maxima are at $\beta_{\text{opt}} = m \times 22.5^\circ$, where m is an integer. These positions are marked with vertical solid lines in Fig. 3. For higher values of F the maxima are shifted from the low intensity positions. The bigger the F parameter is, the bigger the shift of β_{opt} . Using F as a fitting parameter theoretical dependencies are plotted on Fig. 3. The corresponding F fitting parameters for both β experimental curves are $F_{620} = 3.6$ for 620 nm and $F_{310} = 5.76$ for 310 nm. Using the ratio $F_{310}/F_{620} = 1.60$ and the ratio $I_{o,310}/I_{o,620} = 0.60$, we obtain that the product $|\sigma\chi_{xxxx}^{(3)}|$ is 1.33 times higher at 310 nm than at 620 nm.

The main source of error in both intensity and beta dependence measurements is the input intensity measurement uncertainty. We may then conclude that the two estimations for the ratio $(\sigma\chi_{xxxx}^{(3)})_{310}/(\sigma\chi_{xxxx}^{(3)})_{620}$ are in accordance with each other, giving an overall $(\sigma\chi_{xxxx}^{(3)})_{310}/(\sigma\chi_{xxxx}^{(3)})_{620} = 1.28 \pm 10\%$.

$\chi_{xxxx}^{(3)}$ dispersion of BaF_2 as a function of wavelength has been previously investigated by DeSalvo *et al.* [10] using a z -scan measurement at 1064, 532, 355, and 266 nm. By interpolating data in [10] one can estimate $\kappa = (\chi_{xxxx}^{(3)})_{310}/(\chi_{xxxx}^{(3)})_{620} \approx 1.4$. This ratio is comparable with the one reported in this Letter. Furthermore, we can also conclude that the dispersion of σ , the anisotropy of $\chi^{(3)}$, in the spectral range investigated is small and does not exceed the dispersion of $\chi_{xxxx}^{(3)}$.

The method of Boling–Glass–Owyong [11] is frequently used to derive the cubic nonlinearities of ma-

terials from their optical index. Using the Sellmeier equation for optical index dispersion with this model, we can evaluate the dispersion of $\chi_{xxxx}^{(3)}$ for BaF₂. It is then described by

$$\frac{\chi_{xxxx}^{(3)}(\lambda)}{\chi_{xxxx}^{(3)}(\lambda_o)} = \frac{n(\lambda)[n(\lambda)^2 + 2]^2[n(\lambda)^2 - 1]^2}{n(\lambda_o)[n(\lambda_o)^2 + 2]^2[n(\lambda_o)^2 - 1]^2}. \quad (2)$$

Applying Eq. (2) to the wavelengths relevant to our experiment we obtain $(\chi_{xxxx}^{(3)})_{310}/(\chi_{xxxx}^{(3)})_{620} = 1.171$. This estimation is also consistent with the measured value in this work, thereby corroborating the hypothesis that σ presents little dispersion with wavelength.

In conclusion, we demonstrate XPW generation in the UV region and show that the process is six times more efficient than in the visible because of the dispersion of $\chi^{(3)}$. In this work the main goal was to compare XPW generation in the visible and in the UV. Maximum efficiency was 6%, because of unoptimized focusing. With recent discovery of a new more efficient holographic cut [12] one can easily achieve efficiencies between 10% to 20% even with one crystal scheme.

We believe that the results presented here will be useful for extending the XPW nonlinear filter in the UV region and for developing new applications such as pulse characterization and temporal contrast filtering of femtosecond UV pulses. Similar results obtained with LiF crystal at 310 nm show that XPW can be extended to wavelength as low as 266 nm using LiF crystals as it presents a cutoff frequency at 100 nm.

The support of the contracts LaserLab-Europe, RII3-CT-2003-506350, and Extreme Light Infrastructure (grant 212105) and support from the Agence Nationale pour la Recherche through programs

BLAN06-3-134072 (ILAR) and Chaire d'Excellence 2004, are gratefully acknowledged. N. Minkovski, S. Kourtev, and S. Saltiel thank Laboratoire d'Optique Appliquée for their hospitality and support.

References

1. A. Jullien, O. Albert, F. Burgy, G. Hamoniaux, J.-P. Rousseau, J.-P. Chambaret, F. Auge-Rochereau, G. Cheriaux, J. Etchepare, N. Minkovski, and S. Saltiel, *Opt. Lett.* **30**, 920 (2005).
2. V. Chvykov, P. Rousseau, S. Reed, G. Kalinchenko, and V. Yanovsky, *Opt. Lett.* **31**, 1456 (2006).
3. S. S. Bulanov, A. Brantov, V. Yu. Bychenkov, V. Chvykov, G. Kalinchenko, T. Matsuoaka, P. Rousseau, S. Reed, V. Yanovsky, K. Krushelnick, D. W. Litzenberg, and A. Maksimchuk, *Med. Phys.* **35**, 1770 (2008).
4. P. Monot, G. Doumy, S. Dobosz, M. Perdrix, P. D'Oliveira, F. Quéré, F. Réau, and P. Martin, *Opt. Lett.* **29**, 893 (2004).
5. A. Cotel, A. Jullien, N. Forget, O. Albert, G. Cheriaux, and C. L. Blanc, *Appl. Phys. B* **83**, 7 (2006).
6. N. Minkovski, G. Petrov, S. M. Saltiel, O. Albert, and J. Etchepare, *J. Opt. Soc. Am. B* **21**, 1659 (2004).
7. K. Osvay, I. N. Ross, C. J. Hooker, and J. M. D. Lister, *Appl. Phys. B* **59**, 361 (1994).
8. K. Osvay, M. Csataria, A. Gaal, and I. N. Ross, *J. Chin. Chem. Soc. (Taipei)* **47**, 855 (2000).
9. N. Forget, S. Coudreau, F. Lepetit, O. Albert, and T. Oksenhendler, in *Conference on Lasers and Electro-Optics/Quantum Electronics and Laser Science Conference and Photonic Applications Systems Technologies*, OSA Technical Digest Series (CD) (Optical Society of America, 2007), paper CMA3.
10. R. DeSalvo, A. A. Said, D. J. Hagan, E. W. Van Stryland, and M. Sheik-Bahae, *IEEE J. Quantum Electron.* **32**, 1324 (1996).
11. N. Boling, A. Glass, and A. Owyong, *IEEE J. Quantum Electron.* **14**, 601 (1978).
12. L. Canova, S. Kourtev, N. Minkovski, A. Jullien, R. Lopez-Martens, O. Albert, and S. Saltiel, *Appl. Phys. Lett.* **92**, 231102 (2008).